Plant Physiology®

Plant Physiology, 2024, 00, 1–14
https://doi.org/10.1093/plphys/kiae466
Advance access publication 13 September 2024
Research Article

A leucine-rich-repeat receptor-like kinase regulates pollen aperture formation in rice

Xu Zhang,[1,†] Yu-Jin Kim,[2,†] Qian Tan,[1] Ki Hong Jung,[3] Wanqi Liang[1,4,*]

[1]Joint International Research Laboratory of Metabolic & Developmental Sciences, State Key Laboratory of Hybrid Rice, School of Life Sciences and Biotechnology, Shanghai Jiao Tong University, Shanghai 20040, China
[2]Department of Life Science and Environmental Biochemistry, and Life and Industry Convergence Research Institute, Pusan National University, Miryang 50463, Republic of Korea
[3]Graduate School of Green-Bio Science & Crop Biotech Institute, Kyung Hee University, Yongin 17104, Republic of Korea
[4]Yazhou Bay Institute of Deepsea Sci-Tech, Shanghai Jiao Tong University, Sanya 572024, China
*Author for correspondence: wqliang@sjtu.edu.cn
[†]These authors contributed equally.
The author responsible for distribution of materials integral to the findings presented in this article in accordance with the policy described in the Instructions for Authors (https://academic.oup.com/plphys/pages/General-Instructions) is: Wanqi Liang (wqliang@sjtu.edu.cn).

Abstract

Apertures in pollen grains exhibit species-specific patterns and provide an ideal model for studying cell surface patterning. Pollen apertures are critical for cereal crop fertility, and while DEFECTIVE IN APERTURE FORMATION1 (OsDAF1) and INAPERTURATE POLLEN1 (OsINP1) have been documented to participate in pollen aperture formation in rice (*Oryza sativa*), the molecular transduction pathway regulating aperture formation is largely unknown. Here, we report that a leucine-rich-repeat receptor-like kinase (LRR-RLK), APERTURE MISSING1 (AM1), plays a key role in rice pollen aperture formation. Mutations of *OsAM1* lead to complete sterility due to the disappearance of the pollen aperture and failure in pollen tube germination. *OsAM1* encodes a LRR-RLK that belongs to the STRUBBELIG-receptor family. Similar to other reported aperture regulators, OsAM1 assembles to future aperture sites on tetrads after meiosis to regulate aperture formation. The extracellular and intracellular domain of OsAM1 interacts with OsINP1 and OsDAF1, respectively. However, despite their interaction and the absence of aperture formation in *osam1* pollen grains, OsINP1 and OsDAF1 localize to future aperture sites at the tetrad stage. Mutation of *OsINP1*, however, disrupts normal localization of OsAM1, indicating that OsAM1 acts downstream of OsINP1. Our findings reveal the role of a LRR-RLK protein in pollen aperture formation and shed light on the regulatory network of pollen aperture formation.

Introduction

Pollen grains are covered by a robust outer wall called exine (Ariizumi and Toriyama 2011; Quilichini et al. 2015; Shi et al. 2015; Li et al. 2019). In most plant species, exine is not uniformly distributed over the pollen surface, and areas with no exine deposition are defined as pollen apertures. These apertures are important for pollen grains to fold, hydrate, and germinate (Edlund 2004; Furness and Rudall 2004; Katifori et al. 2010; Vieira and Feijó 2016; Albert et al. 2018; Li et al. 2018; Zhou and Dobritsa 2019; Zhang et al. 2020), and the numbers, shapes, and locations of pollen apertures are a major morphological feature across different species. Two of the most typical patterns are displayed by the model dicot *Arabidopsis* (*Arabidopsis thaliana*) and the model monocot rice (*Oryza sativa*) (Just and Wodehouse 1936). *Arabidopsis* pollen apertures are 3 long furrows, equally spaced along the pollen surface, while the rice pollen aperture is a single, distal pore with decorations such as annulus and operculum (Köhler and Lange 1979; El-Ghazaly and Jensen 1986; Dobritsa and Coerper 2012). The strict, but disparate, patterning of pollen apertures in these model species provides an excellent system in which to study cell surface patterning.

Pollen apertures start to form at the tetrad stage, just after the meiosis. A tetrad comprises 4 newly formed microspores, generated through 2 rounds of meiotic cell division, surrounded by a thick callose wall. Defined areas of the microspore plasma membrane (PM) stay close to the callose wall to prevent exine deposition and eventually form apertures (Mccormick 2004; Ma 2005; Zhang et al. 2011; Wang and Dobritsa 2018). Several proteins have been reported to participate in this process. In *Arabidopsis*, INAPERTURATE POLLEN1 (AtINP1) and AtINP2 form a species-specific protein complex that excludes specific membrane domains from exine deposition. AtINP1 localizes to future aperture sites, while AtINP2 localization remains unknown (Dobritsa and Coerper 2012; Dobritsa and Reeder 2017; Dobritsa et al. 2018; Li et al. 2018; Lee et al. 2021). The protein kinase AtD6PKL3 (D6 PROTEIN KINASE-LIKE3) is also involved in pollen aperture formation, required for correct localization of AtINP1 and vice versa although no direct interaction has been detected between the 2 proteins (Lee et al. 2018). Moreover, ELMOD family proteins (MCRs; MACARON) and a yet unidentified mutant *doughnut* (*dnt*) have been reported to determine numbers, positions, and shapes of apertures but do not localize to aperture sites or interact with other aperture determinants (Plourde et al. 2019; Zhou and Dobritsa 2019; Zhou et al. 2021). In rice, OsINP1 is required for the formation of the aperture, as well as the surrounding annulus and operculum. A lectin receptor-like kinase, Defective in Aperture Formation1 (DAF1), interacts with OsINP1 for annulus formation. Both OsDAF1 and OsINP1 localize to future aperture

Received March 18, 2024. Accepted August 6, 2024.

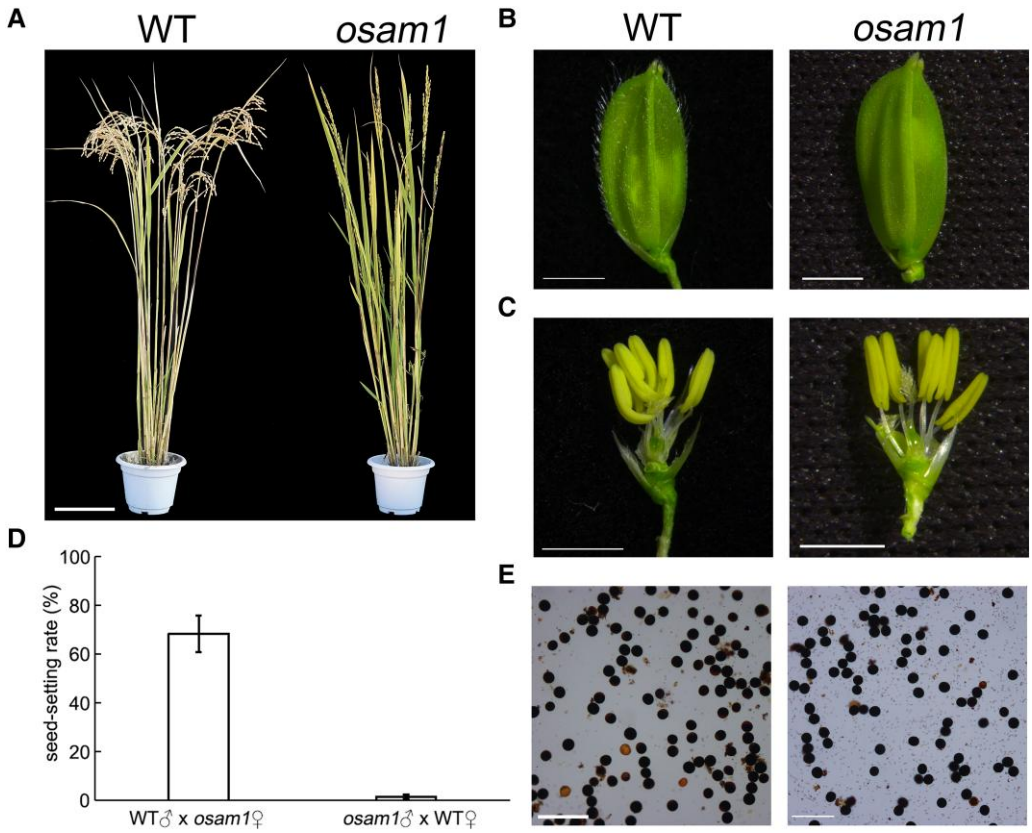

Figure 1. Mutation of *OsAM1* leads to male sterility. **A** to **C)** Comparisons of mature plants **A)**, spikelets **B)**, and anthers **C)** for WT and *osam1* T-DNA mutant. **D)** Seed-setting rate of indicated plants crossed with indicated pollens. For each line, 5 panicles from independent plants were pollinated. Data show mean ± SD. **E)** Pollen grains stained by I_2–KI from WT and *osam1* T-DNA mutant. Images in **A)** were digitally extracted for comparison. The phenotypes were observed at least 3 times independently with similar results. Scale bars: 10 cm **A)**; 2 mm **B**, **C)**, and 200 μm **E)**.

sites; OsINP1 is required for correct OsDAF1 localization, but not vice versa (Zhang et al. 2020). However, what initiates the specific localization of pollen apertures and how is the developmental signal pathway conducted are largely unknown.

LRR-RLKs are a large set of transmembrane receptor proteins that regulate many aspects of plant biological processes by mediating signal transduction from extracellular to intracellular spaces (Shiu and Bleecker 2001; Afzal et al. 2008; De Smet et al. 2009; Tor et al. 2009); to date, they have not been implicated in pollen aperture formation. Here, we report that an LRR-RLK gene, *Aperture Missing1* (*AM1*), participates in pollen aperture formation in rice. We demonstrate that the loss of AM1 function leads to the disappearance of the pollen aperture, causing sterility in rice. OsAM1 localizes to the future aperture sites during the tetrad stage and interacts with OsINP1 and OsDAF1. Genetic evidence indicates that AM1 acts downstream of OsINP1 in pollen aperture development, and the polarized distribution of OsDAF1 is partially relied on AM1 functioning. Our study thus reveals a novel function for the widespread LRR-RLK protein family in pollen aperture formation.

Results

Osam1 is a male sterile mutant without pollen aperture

A sterile line was isolated from a previously described rice T-DNA insertion library (Jeon et al. 2000). Due to the pollen aperture phenotype described below, we named it *am1*. *osam1* displayed complete sterility (Fig. 1A). The development of spikelet and floral organs looked normal when compared with the wild type (WT) (Fig. 1, B and C). *osam1* was able to set seeds when pollinated with WT pollen grains; on the contrary, WT plants pollinated with mutant pollen grains were completely sterile (Fig. 1D), indicating that *osam1* is defective in male reproduction. However, semithin section analysis showed a normal development of the anther and pollen in *osam1* (Supplementary Fig. S1). Furthermore, iodine staining results showed mature pollen grains in the mutant anther (Fig. 1E) similar to those in WT, implicating defects in pollen tube germination, growth, and/or fertilization.

We further analyzed the pollen germination and found that *osam1* pollen grains were unable to germinate neither in vitro nor in vivo despite normal starch accumulation (Fig. 2, A and B). Scanning electron microscopic (SEM) observations showed that although the pollen exine development was normal, *osam1* completely lacked pollen apertures (Fig. 2C). These results indicate that OsAM1 participates in rice pollen aperture formation.

OsAM1 encodes an LRR-RLK required for rice pollen aperture formation

PCR and sequencing analysis located the T-DNA insertion in the coding region of LOC_Os02g10110, which encodes a 757 aa protein belonging to the LRR-RLK family (Fig. 3, A and B). Like other typical LRR-RLK proteins, OsAM1 comprises an N-terminal signal peptide, an extracellular leucine-rich-repeat (LRR) domain, a transmembrane region, and a serine/threonine protein kinase domain at the C-terminus. In addition, an extra potential hydrophobic region (eHR) is present between the signal peptide and LRR domain (Fig. 3B).

To verify that this is the causative gene for the observed phenotype, we used CRISPR-Cas9 gene editing to generate 2 more

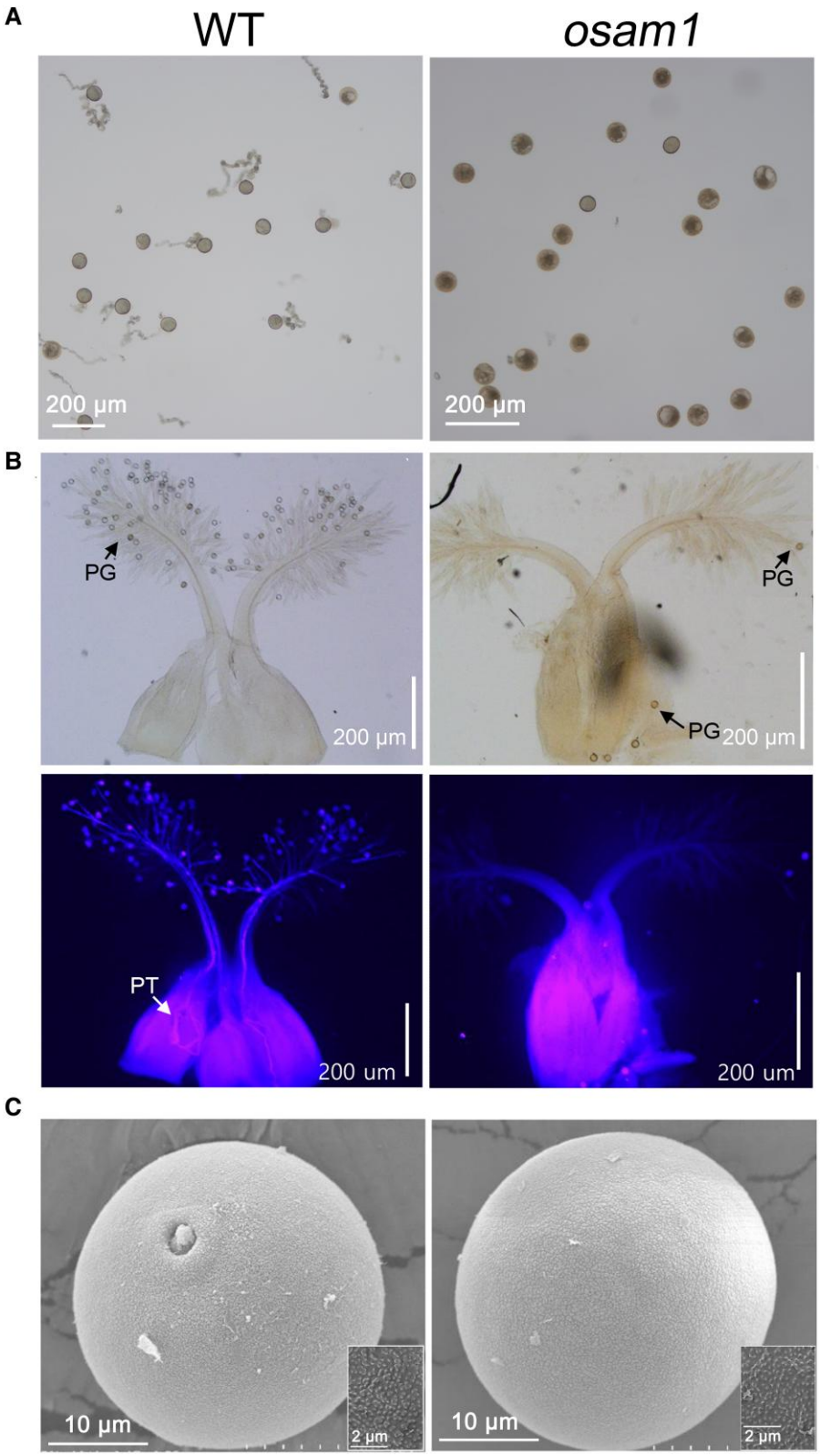

Figure 2. *OsAM1* participates in rice pollen aperture formation. **A**, **B**) In vitro and in vivo pollen germination of WT and *osam1* pollen. In vitro **A)** and in vivo **B)** pollen germination assays of WT rice and *osam1*. PG, pollen grain. PT, pollen tube. **C)** Pollen grain and exine (inset) SEM of WT and *osam1* T-DNA mutant. The phenotypes were observed at least 3 times independently with similar results.

LOC_Os02g10110 alleles, with a premature stop codon after 134 or 503 aa (Fig. 3, A and B). The lines carrying these mutations, *aperture missing1*^{cas9} (*am1*^{cas9}) and *aperture missing1*$^{cas9-1}$ (*am1*$^{cas9-1}$), displayed the same phenotype as the T-DNA insertion allele: complete male sterility but seemingly normal vegetative growth, flower, anther, and pollen development, but missing the pollen aperture (Fig. 3, C to G). For complementation experiments, we transformed the WT *OsAM1* genomic DNA (gDNA) driven by the

native promoter (fused with YFP) into the *osam1*^{cas9} mutant (*OsAM1gDNA-YFP osam1*^{cas9}). All 52 T_0 transformants displayed restored fertility and WT pollen aperture phenotypes (Fig. 3, C to G), confirming that *OsAM1* is the causative gene for the aperture defect. Expression of an OsAM1–GFP fusion construct in *Nicotiana benthamiana* epidermal cells, as well as a plasmolysis assay, confirmed that OsAM1 localizes to the PM (Supplementary Fig. S2).

OsAM1 belongs to SRF

OsAM1 is annotated as a STRUBBELIG-receptor protein in rice, named after the eponymous SUB homolog from *Arabidopsis*. The STRUBBELIG-receptor family (SRF) includes SUB and SRF1 to 8, in which SUB, SRF3, and SRF4 have been reported to be involved in organ morphogenesis or callose deposition during defense responses (Chevalier et al. 2005; Kwak et al. 2005; Eyüboglu et al. 2007; Alcázar et al. 2010; Vaddepalli et al. 2011; Lin et al. 2012; Gao et al. 2019; Platre et al. 2022). To perform the phylogenetic analysis of OsAM1, we retrieved 273 protein homologs belonging to 44 plant species for phylogenetic analysis (Fig. 4; Supplementary Table S1). SRFs were found across the plant kingdom, from mosses to higher eudicots, with 1 to 10+ homologs present in most species ($E < e^{-60}$, or hit score > 300); in algae, only proteins with low similarities were found ($E > e^{-40}$ or hit score < 160). Phylogenetic analysis reveals that SRF proteins cluster into 5 clades: the SUB-SRF1/3 clade, SRF8 clade, SRF6/7 clade, SRF4/5 clade, and SRF2 clade, based on nomenclature from *Arabidopsis* (Fig. 4). Algal sequences remain outside this taxonomy, suggesting that SRF proteins likely emerged after algal species differentiation. Furthermore, the SUB-SRF1/3 clade includes sequences from mosses and ferns while the other 4 clades typically only contain angiosperm sequences, indicating that SUB, SRF1, and SRF3 are evolutionarily more fundamental in plants. OsAM1 was found to belong to the SRF2 clade (Fig. 4; Supplementary Table S1), and grass SRF2 putative orthologs share higher similarity with OsAM1 (>80%) than AM1 homologs from other species (30% to 60%; Supplementary Table S1).

OsAM1 localizes to future aperture sites in rice tetrads

Most proteins so far reported to be involved in pollen aperture formation, including OsINP1 and OsDAF1 in rice, localize to the future aperture sites in tetrads to facilitate aperture initiation and development (Dobritsa and Coerper 2012; Lee et al. 2018; Zhang et al. 2020). To explore whether OsAM1 displays a similar localization pattern, we used the *osam1*^{cas9} complementation line described above to monitor YFP-tagged OsAM1 protein distribution in the anther. Similar to the previously reported lectin-RLK OsDAF1 (Zhang et al. 2020), OsAM1 localized in the PM and cytosol of microspore mother cells during meiotic stage 7 (Fig. 5A). OsAM1 remains diffused both in the PM and cytoplasm in dyads (Fig. 5B) and newly formed tetrads (Fig. 5C). As tetrad development continues, OsAM1 starts to accumulate at 4 distal sites (Fig. 5D), eventually assembling into prominent foci that mark future aperture sites of microspores (Fig. 5E). After degradation of callose wall and release of 4 microspores from the tetrad, the OsAM1-YFP signal remains clearly at aperture sites (Fig. 5F). These results demonstrate that OsAM1 locates to future aperture sites to facilitate aperture development during tetrad stage.

OsAM1 acts downstream of OsINP1 in pollen aperture development

To evaluate the relationship between OsAM1 and other proteins known to contribute to rice pollen aperture development (OsINP1 and OsDAF1), we performed yeast 2 hybrid (Y2H), bimolecular fluorescence complementation (BiFC), and split-luciferase analysis. Constructs expressing truncated OsAM1 containing the N-terminus extracellular domain between the eHR and the transmembrane domain (OsAM1-N) or the intracellular domain (OsAM1-C) were used for protein interaction assays (Supplementary Fig. S3). We found that the extracellular domain of OsAM1 was able to interact with OsINP1 in yeast (Fig. 6A). This interaction was further confirmed by BiFC and split-luciferase experiments in tobacco cells (Fig. 6, B and C).

To further explore the relationship between OsAM1 and OsINP1, we transformed *OsAM1gDNA-YFP* into the *osinp1* mutant (Zhang et al. 2020). OsAM1 did not localize to future aperture sites in *osinp1* mutant tetrads (Fig. 7A, upper panel). To confirm this result, we backcrossed the *OsAM1gDNA-eYFP;osinp1* lines with WT to generate heterozygous *osinp1−/OsINP1+* plants expressing *OsAM1gDNA-YFP*. In the heterozygotes, OsAM1 localized correctly to future aperture sites in tetrads (Fig. 7A, lower panel). These findings suggest that proper localization of OsAM1 is dependent on functional OsINP1.

We subsequently investigated how the mutation of *OsAM1* affects localization of OsINP1 by introducing *OsINP1-eYFP* (Zhang et al. 2020) into *osam1*^{cas9}. To our surprise, although no aperture was developed in *osam1*^{cas9} pollen, localization of OsINP1 was not affected at all, still able to correctly assemble to future aperture sites in the tetrad (Fig. 7B).

These findings suggest that the accumulation of OsINP1 at future aperture sites does not rely on OsAM1 but that OsINP1 is required for correct localization of OsAM1 to initiate the aperture formation. Generating a further double mutant (*osam1*^{cas9}*;osinp1*) revealed no additive phenotype compared with either single mutant (Supplementary Fig. S4). Given these results, we propose that OsAM1 acts downstream of the OsINP1 in pollen aperture development.

OsDAF1 interacts with OsAM1, and its localization is facilitated but not entirely determined by OsAM1 function

We next measured the relations between OsDAF1 and OsAM1 by protein interaction assay. Y2H, BiFC, and split-luciferase assays demonstrated that intracellular domain of OsAM1 was able to interact with intracellular OsDAF1 (truncated as in Zhang et al. 2020) (Fig. 8, A to C). To further investigate the relation between OsAM1 and OsDAF1, we transformed the *OsDAF1-eYFP* (Zhang et al. 2020) into the *osam1*^{cas9} line to detect the impact of *OsAM1* mutation on OsDAF1 distribution. In a result, OsDAF1 was still able to partially localize to future aperture sites in the *osam1*^{cas9} tetrad, with a less concentrated signal compared to OsDAF1 in WT tetrads (Fig. 9). Based on previous report that OsINP1 is able to recruit OsDAF1 (Zhang et al. 2020), and the result above that normal localization of OsINP1 was not affected in *osam1* mutants (Fig. 7B), we speculate that interaction between OsDAF1 and OsAM1 is beneficial but not decisive for complete assembling of OsDAF1 on future aperture sites.

Our previous results indicate that OsINP1 interacts with the intracellular domain of OsDAF1. This study shows that OsINP1 also interacts with the extracellular domain of OsAM1. We propose that OsINP1 may interact with OsAM1 and OsDAF1 via different regions. To verify this possibility, we performed Y2H of truncated OsINP1 to determine which region interacts with extracellular OsAM1 or intracellular OsDAF1. OsINP1 is a 232 aa protein containing a DOG1 domain at 36 to 119 aa. Therefore, we created 3 different truncations:

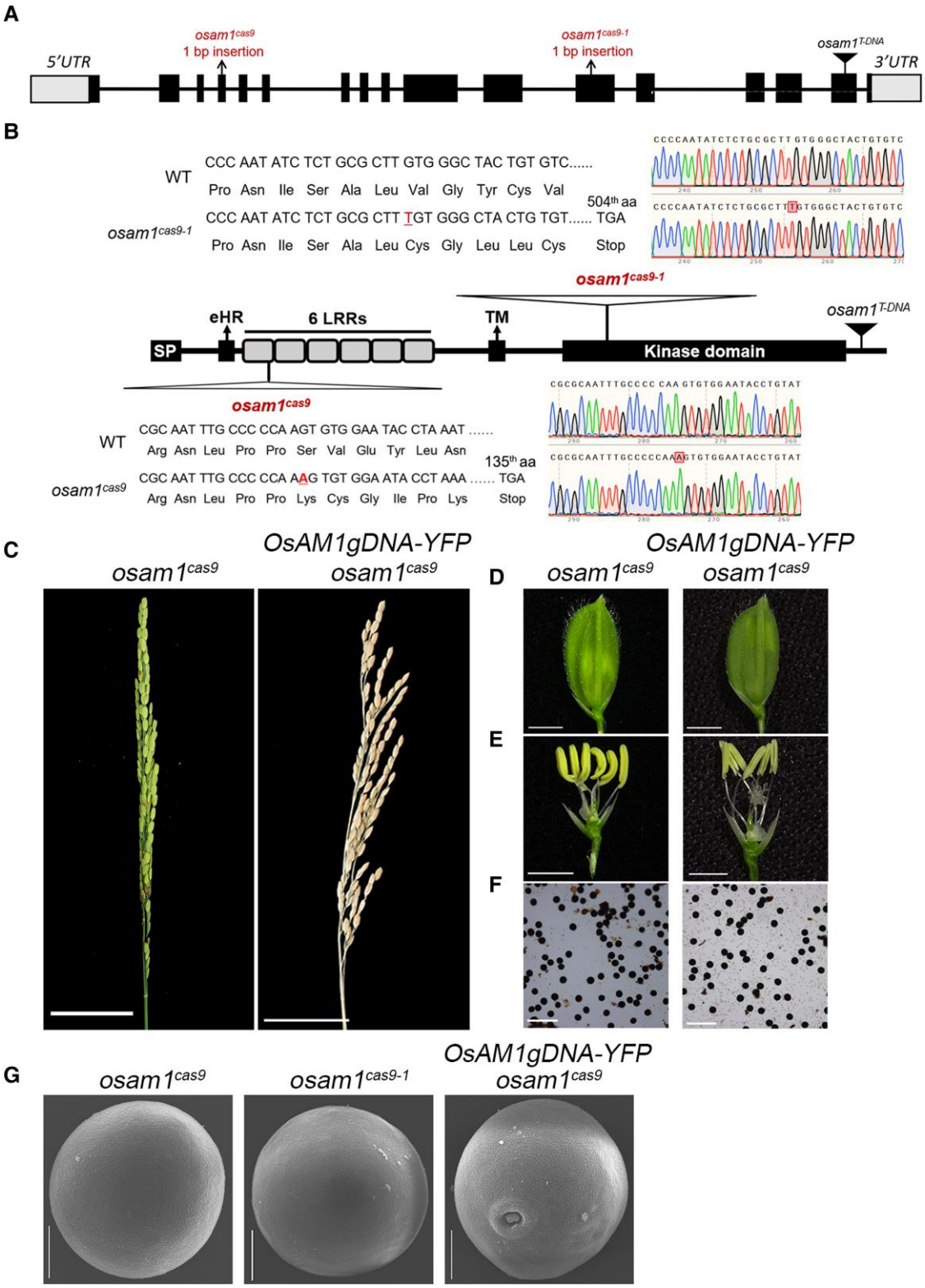

Figure 3. OsAM1 encodes an LRR-RLK required for rice pollen aperture formation. **A)** Schematic diagram of the *OsAM1* gene, showing the T-DNA insertion site and $osam1^{cas9}$ and $osam1^{cas9-1}$ mutation sites. Gray boxes indicate UTRs, black boxes indicate exons, and black lines indicate introns. **B)** Schematic diagram of putative OsAM1 protein domains, again showing mutation sites. SP, signal peptide; eHR, extra potential hydrophobic region; LRR, leucine rich repeat region; TM, transmembrane domain. **C to F**) Comparison of spikelets **C)**, flowers **D)**, anthers **E)**, and mature pollen grains by I_2–KI staining (**F**; deep staining indicates starch accumulation in pollen) for $osam1^{cas9}$, and $osam1^{cas9}$ rescued by complementation with genomic *OsAM1* sequence fused with YFP (*OsAM1gDNA-YFP* $osam1^{cas9}$). **G)** Pollen SEM of $osam1^{cas9}$, $osam1^{cas9-1}$, and $osam1^{cas9}$ complementation lines. The phenotypes were observed at least 3 times independently with similar results. Scale bars: 5 cm **C)**, 2 mm **D**, **E)**, 200 μm **F)**, and 10 μm **G)**.

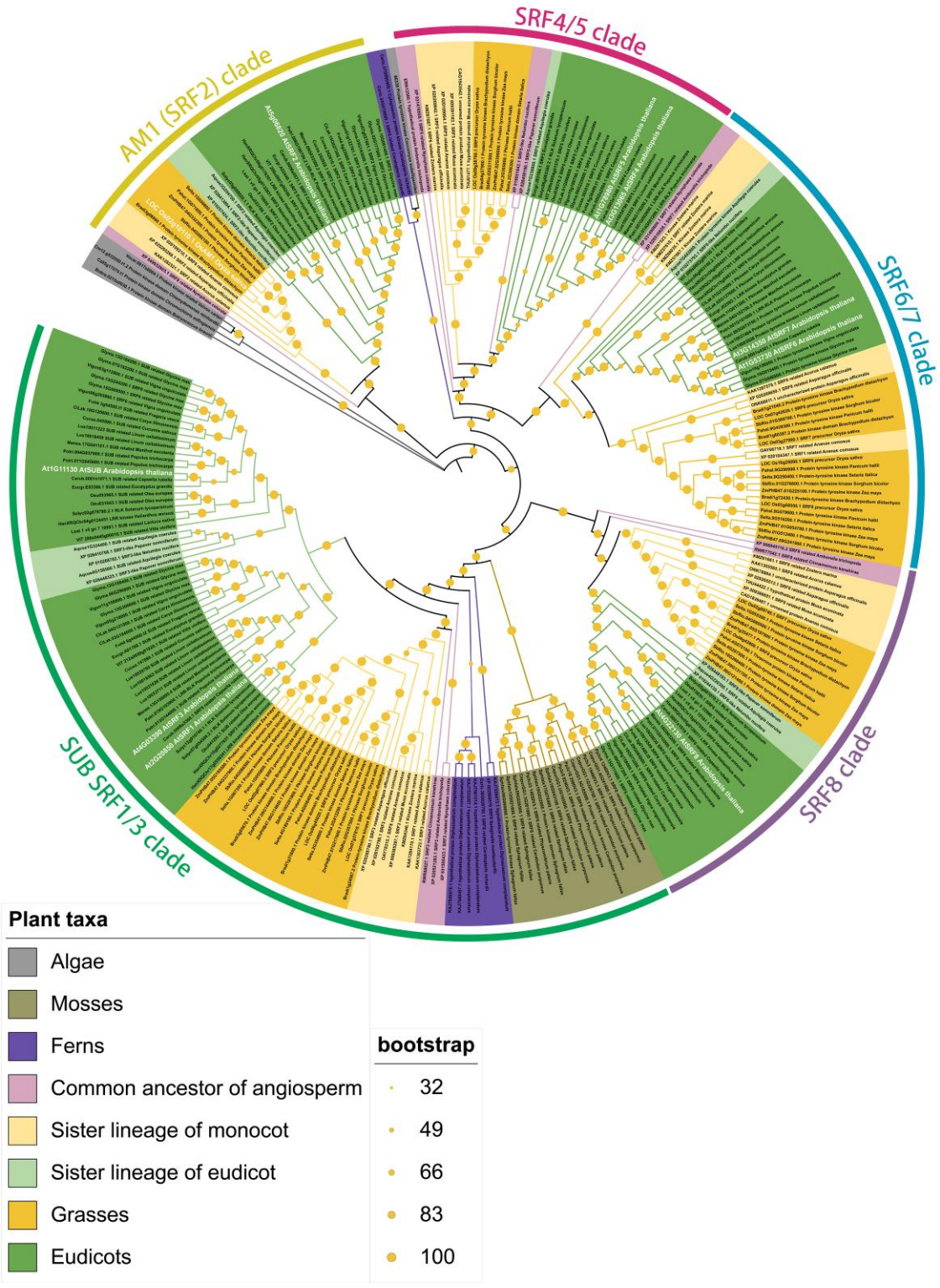

Figure 4. OsAM1 belongs to the SRF2 clade of the SRF gene family. Maximum likelihood phylogenetic tree of SRF proteins from a variety of plant taxa (indicated by color coding), with 5 clades indicated. Orange circles: bootstrap values. Details of accession numbers, identities to OsAM1, and blast score of sequences are in Supplementary Table S1.

(i) OsINP1ΔN (36 to 232 aa); (ii) OsINP1ΔC (1 to 119 aa); and (iii) OsINP1ΔN + DOG1 (119 to 232 aa) (Supplementary Fig. S5A). We found that N-terminus region of OsINP1 is important for its interaction with OsAM1-N, whereas C-terminus region of OsINP1 is critical for interacting with OsDAF1-C (Supplementary Fig. S5, B and C).

Discussion

The strict, species-specific control of pollen aperture patterning suggests the involvement of various signal transduction pathways during pollen aperture development. Here, we provide evidence

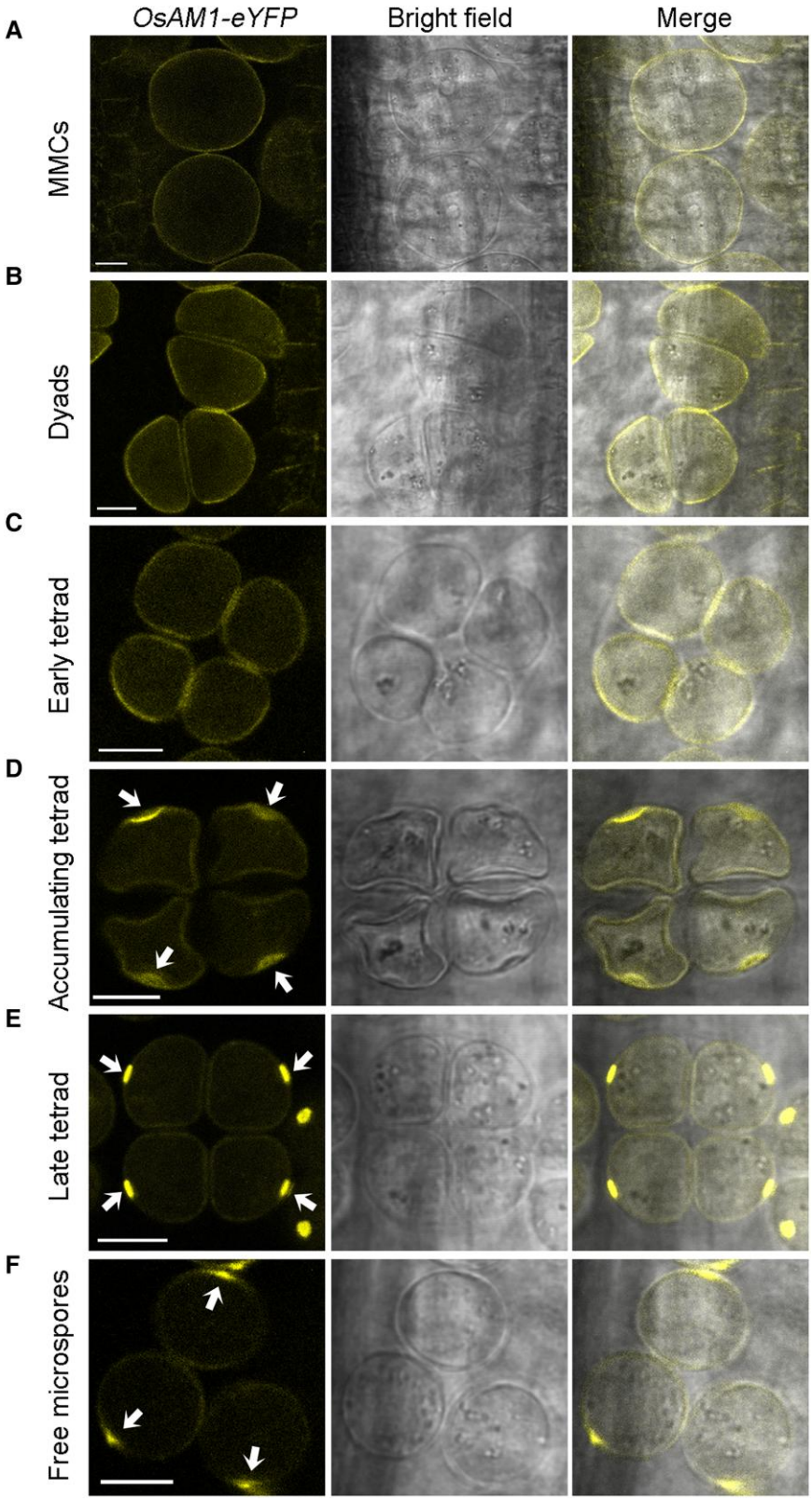

Figure 5. OsAM1 localizes to future aperture sites. **A to F**) Confocal and merged bright-field imaging of *OsAM1:gOsAM1-eYFP* plant anthers or microspores at different developmental stages. White arrows indicate the future aperture sites on tetrads or free microspores. These localizations were observed in 3 independent lines with similar results. Scale bars: 10 μm.

for the involvement of an LRR-RLK family protein in pollen aperture formation.

Several proteins have been shown to work together, directly or indirectly, to determine or facilitate pollen aperture development in *Arabidopsis* and rice. AtINP1 was the first, a protein of unknown function reported back in 2012; in more recent research, it has been shown to directly interact with AtINP2 to function in a species-specific manner (Dobritsa and Coerper 2012; Dobritsa

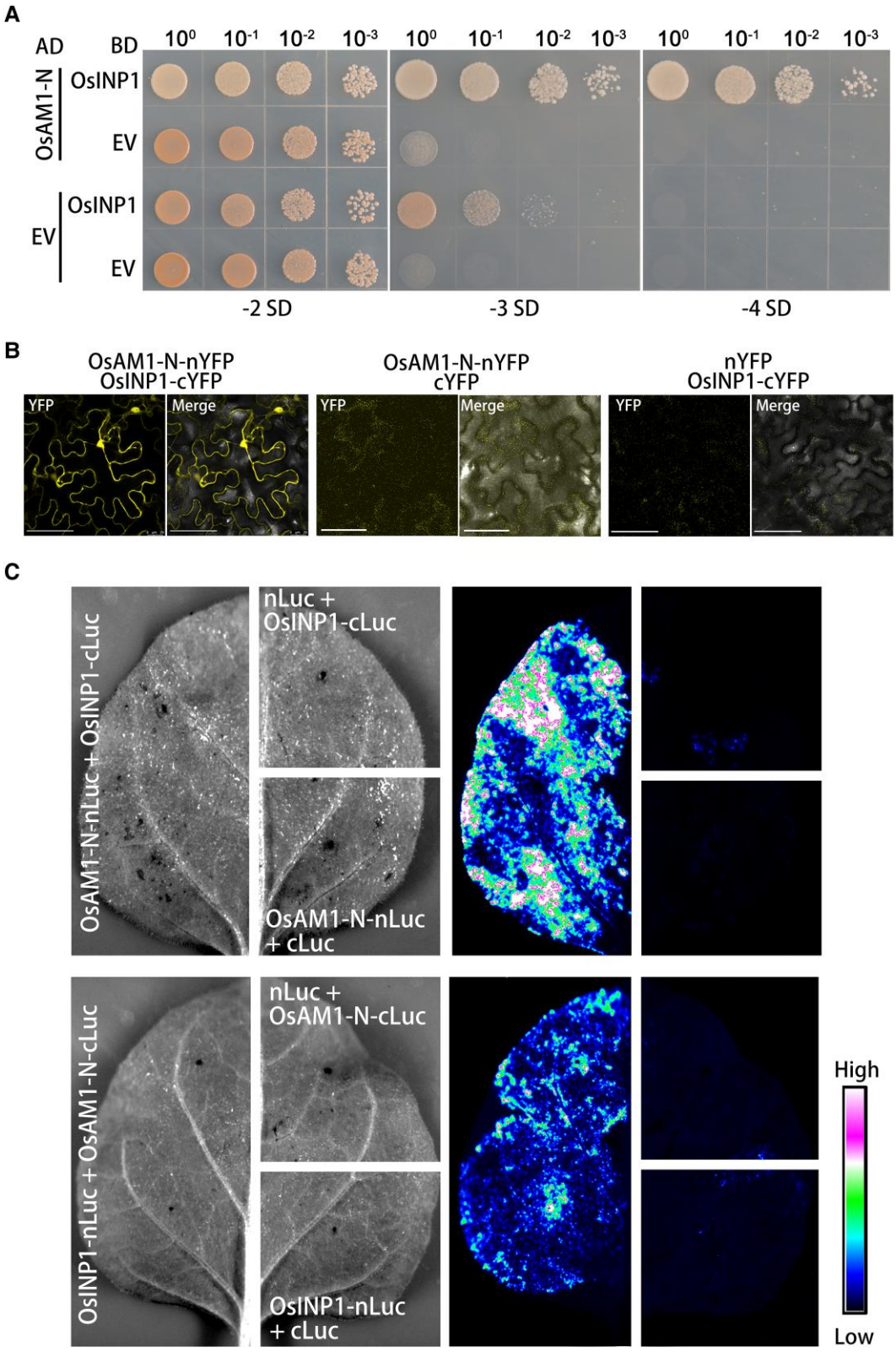

Figure 6. Extracellular domain of OsAM1 physically interacts with OsINP1. **A)** Y2H assay between OsAM1-N and OsINP1. AD, activating domain; BD, DNA-binding domain; EV, empty vector; −2/−3/−4 SD, synthetic defined medium without Leu/Trp, Leu/Trp/His, or Leu/Trp/Ade/His. **B)** BiFC assay between OsAM1-N and OsINP1 in tobacco leaf cells. nYFP, N-terminal yellow fluorescent protein; cYFP, C-terminal yellow fluorescent protein. **C)** Split-luciferase assays between OsAM1-N and OsINP1 with controls. cLuc, C-terminal luciferase; nLuc, N-terminal luciferase. Similar results were observed at least 3 times independently. Scale bars: 75 μm.

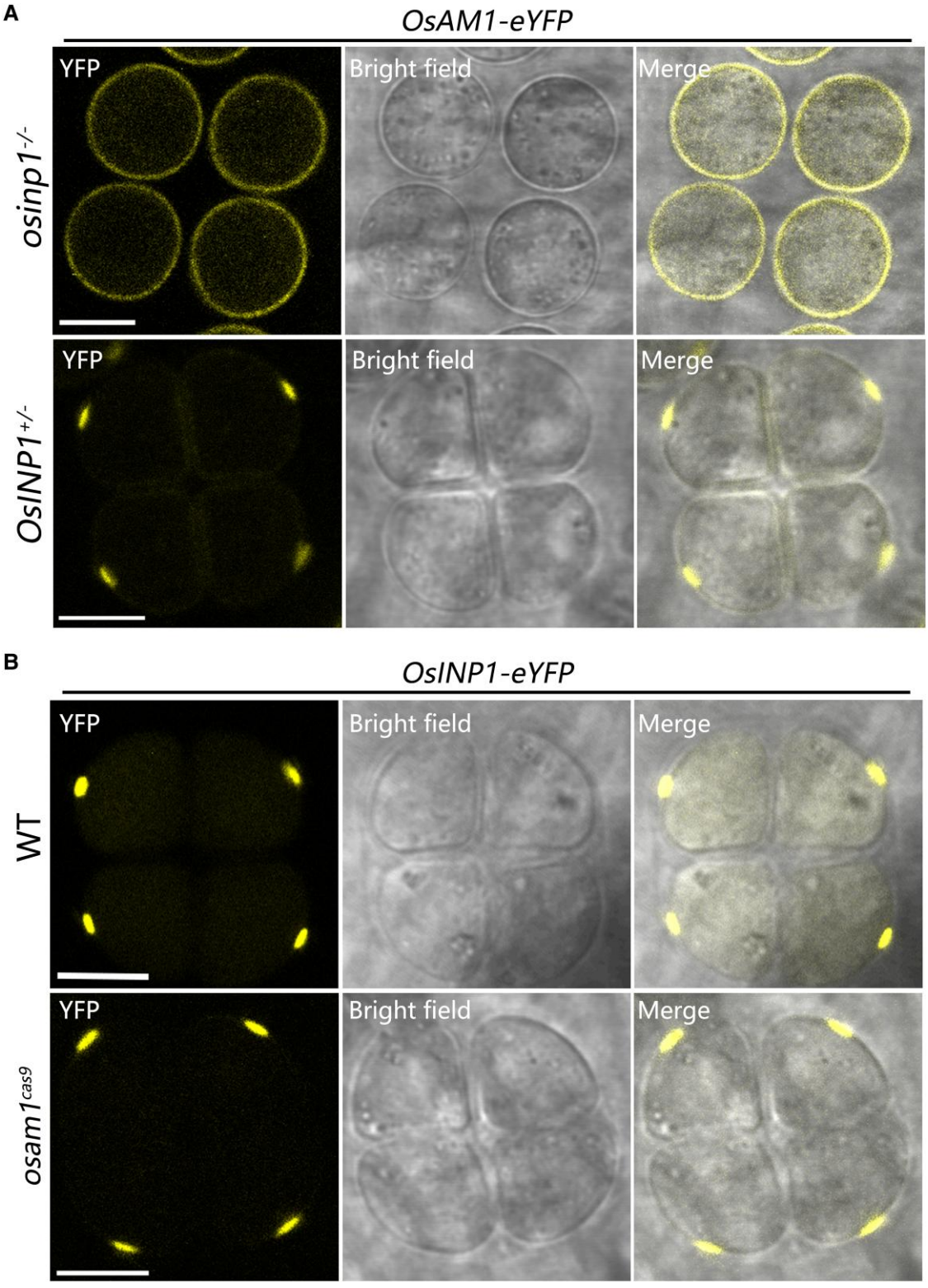

Figure 7. OsINP1 is required for the recruitment of OsAM1 to the future aperture but not vise versus. **A)** Confocal and merged bright-field images of OsAM1-eYFP localization in a tetrad of heterozygous *OsINP1*$^{+/-}$ or homozygous *osinp1*$^{-/-}$. **B)** Confocal and merged bright-field images of OsINP1-eYFP localization in WT and *osam1*^{cas9} tetrad. Similar results were observed at least 3 times independently. Scale bars: 10 μm.

and Reeder 2017; Dobritsa et al. 2018; Li et al. 2018; Lee et al. 2021). Sequences of INP1 and INP2 homologs are highly diversified across flowering plants, suggesting that diverse interactors or mechanisms of action may exist in different species (Lee et al. 2021). For example, tomato INP1 (SlINP1) is not able to substitute for the loss of *Arabidopsis* INP1 but can promote aperture formation in *Arabidopsis* when coexpressed with its partner SlINP2. AtINP1 and AtINP2 have been defined as late-acting aperture factors recruited to the future aperture sites on the PM (Lee et al. 2021). In rice, OsINP1 was reported to interact with OsDAF1 to

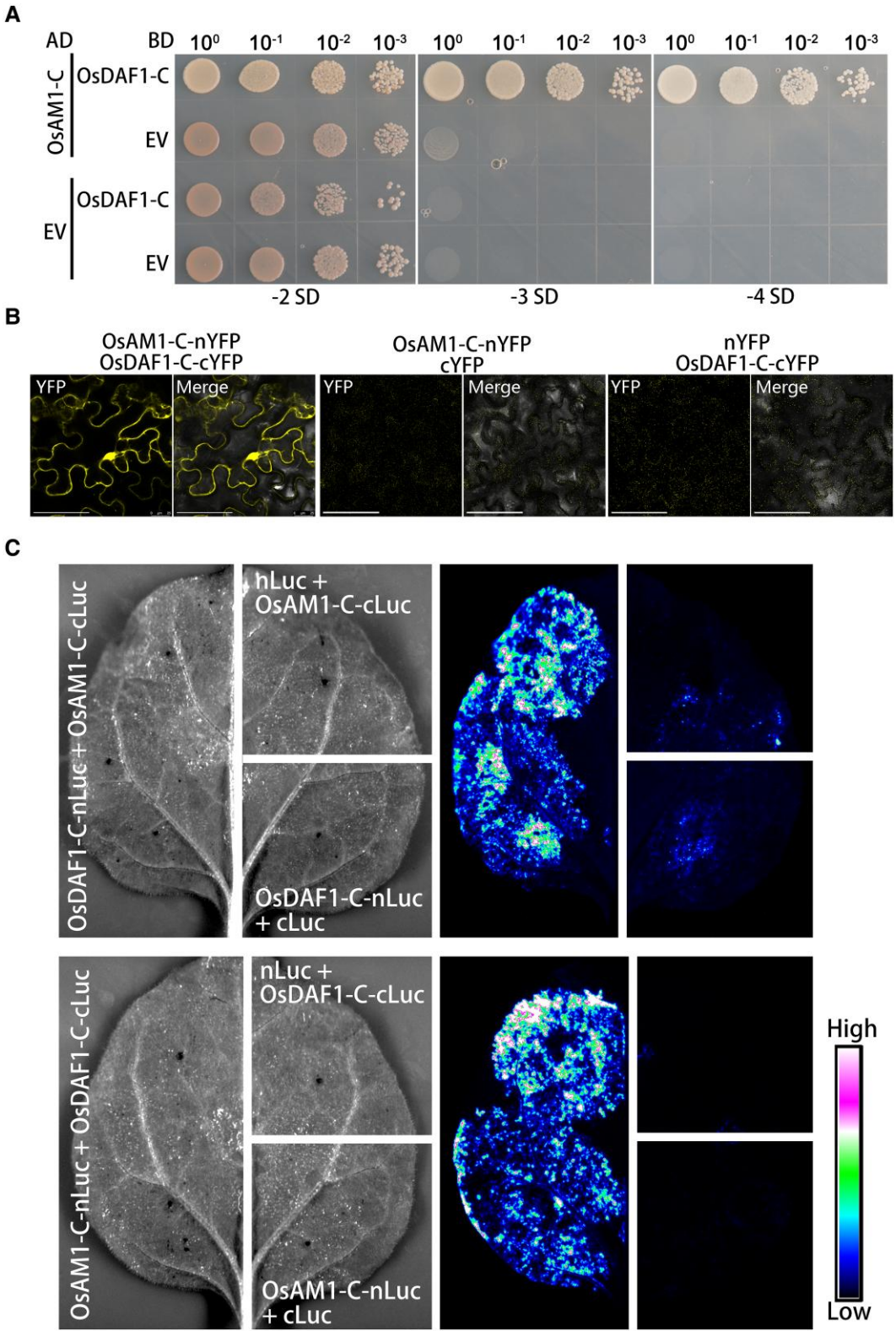

Figure 8. Intracellular domain of OsAM1 and OsDAF1 interacts with each other. **A)** Y2H assay between OsAM1-C and OsDAF1-C. AD, activating domain; BD, DNA-binding domain; EV, empty vector; −2/−3/−4 SD, synthetic defined medium without Leu/Trp, Leu/Trp/His, or Leu/Trp/Ade/His. **B)** BiFC assay between OsAM1-C and OsDAF1-C in tobacco leaf cells. nYFP, N-terminal yellow fluorescent protein; cYFP, C-terminal yellow fluorescent protein. **C)** Split-luciferase assays between OsAM1-C and OsDAF1-C with controls. cLuc, C-terminal luciferase; nLuc, N-terminal luciferase. Scale bars: 75 μm.

determine the development of the annulus structure in the pollen aperture (Zhang et al. 2020). Our study showed that OsAM1 interacts with both OsINP1 and OsDAF1 via different domains (Figs. 6 and 8). INP1 and its orthologs contain no obvious transmembrane domain but may accumulate on different sides of the PM. Evidence from plasmolyzed tetrads shows that AtINP1 resides in the callose wall, which surrounds the PM at the tetrad stage (Dobritsa et al. 2018), while OsINP1 is presumed to be present

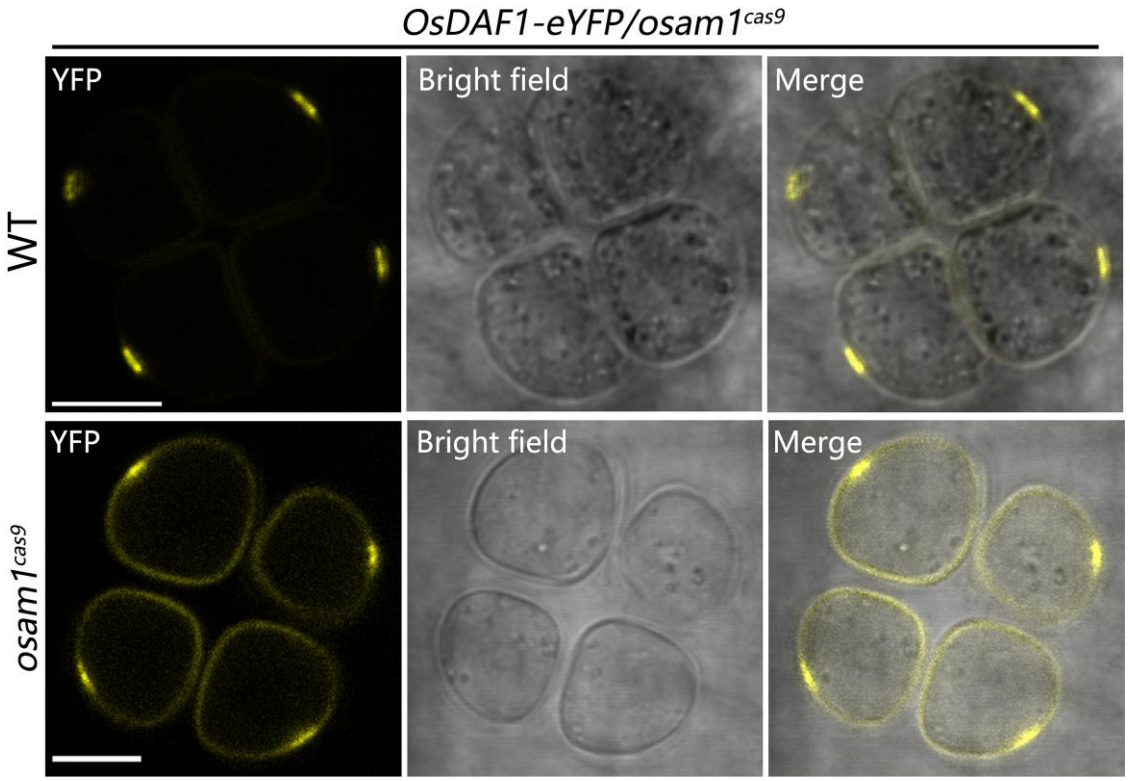

Figure 9. Normal localization of OsDAF1 is facilitated by OsAM1. Confocal and merged bright-field images of OsDAF1-eYFP localization in WT and *osam1*^{cas9} tetrads. Similar results were observed at least three times independently. Scale bars: 10 μm

intracellularly based on its interaction with the intracellular C-terminal region of OsDAF1 (Zhang et al. 2020). In this study, we observed that OsINP1 physically interacts with the extracellular domain of OsAM1 (Fig. 6, A to C), indicating that OsINP1 might appear on both sides of the PM. We found that N-terminus region of OsINP1 is important for its interaction with OsAM1-N, whereas C-terminus region of OsINP1 is indispensable for interacting with OsDAF1-C (Supplementary Fig. S5, B and C). These observations supported the speculation that OsINP1 appears at both sides of the PM in rice, and its ability to interact with both extracellular and intracellular factors through distinct domains underscores its pivotal role in pollen aperture formation.

Protein localization analysis indicated that while the *osinp1* mutation led to incorrect protein localization of OsAM1 (Fig. 7A) and OsDAF1 (Zhang et al. 2020), OsINP1 and OsDAF1 could fully or partially assemble to the future aperture sites in *osam1* tetrads, even though an aperture was not formed (Figs. 7B and 9). Based on the physical and genetic interaction of these aperture players, we proposed that OsINP1 acts earlier than other known aperture factors in rice. OsAM1 functions downstream of OsINP1 and is recruited to the future aperture sites by OsINP1; therefore, its absence does not affect the correct localization of OsINP1 (Fig. 7B). On the other hand, OsAM1 is involved in recruiting other components required for aperture formation. Mutation of *OsAM1* dampened the normal assembly but not abolished the aperture localization of OsDAF1. It is likely that OsDAF1 is recruited by the joint efforts of OsINP1 and OsAM1 to the proposed annulus area next to the aperture gap, where the active kinase OsDAF1 could promote annulus development and together form the intact grass pollen aperture structure.

Pollen apertures are associated with areas on tetrads where callose cell wall degradation is slower and remains close to the PM to prevent exine formation. Therefore, proteins related to callose synthesis, deposition, or degradation are highly likely to be involved in pollen aperture development. AM1 belongs to the SRF family, of which SUB is presumed to not only localize to the PM, but also present at plasmodesmata where it participates in cell wall damage responses that often involve callose accumulation (Chaudhary et al. 2020). SRF3 has also been shown to localize to both the PM and plasmodesmata and play a role in root growth, iron homeostasis, and immunity pathways via regulating callose synthases (Platre et al. 2022). In our study, we found that loss of OsAM1 function in rice leads to the disappearance of the aperture and indicates that AM1 may also play a role in callose metabolism. Further investigation of whether and how AM1 regulates callose metabolism could provide insights into the mechanism underlying aperture patterning. Canonical LRR-RLK proteins contain 2 typical hydrophobic regions, a signal peptide at N-terminal end, and a transmembrane domain at the middle of LRR and kinase domain. However, multiple algorithms predicted the existence of an extra potential hydrophobic region (eHR) in OsAM1 between the signal peptide and the LRR domain (Supplementary Fig. S6; Fig. 3B). As mentioned above, AM1 proteins belong to SRFs, but OsAM1 was the only SRF in rice that contained the eHR (Supplementary Fig. S6). Furthermore, most AM1 ortholog proteins in other grass species also contain the distinct eHR (Supplementary Fig. S7), whereas SRF2 proteins from eudicot plants do not (Supplementary Fig. S8). These data suggest that grass AM1 proteins share a unique eHR between the signal peptide and LRR domain. Further study in this domain might help to uncover the mechanism underlying the species-specific pollen aperture pattern.

Materials and methods

Plant materials and growth conditions

Rice (*O. sativa*) plants were grown in the paddy field at the Shanghai Jiao Tong University during the natural growing season

as described (Zhang et al. 2020). The WT line used for all analyses was *O. sativa* ssp. japonica, cv. Dongjing.

Imaging and microscopy

Morphological images of whole rice plants were captured with a Nikon E995 digital camera. Pictures of flowers were photographed with a Leica M205A microscope. For pollen viability analysis, anthers were immersed into Lugol's iodine (I_2–KI) solution and crushed with tweezers; released pollen grains were photographed with a Nikon Eclipse 80i microscope.

For SEM observations, rice flowers were fixed in formaldehyde/acetic acid/ethanol solution for 2 h, dehydrated with a 70, 80, 90, 95, and 100% (*v*/*v*) ethanol series and dried using a Leica EM CPD300 automated critical dryer. Rice pollen was released on electric conductive adhesive tape and coated with gold particles using a cool sputter coater (Leica EM SCD005). Pollen grain surfaces were photographed under a scanning electron microscope (Hitachi S3400N, Tokyo, Japan).

For imaging rice microsporocytes via confocal microscopy, Stage 7 to 9 anthers were placed into 20% glycerol on a slide for microscopy. Fluorescent signals of eYFP were monitored using a Leica SP8 confocal microscope (Leica TCS SP8 X, excitation 514 nm; emission 522 to 555 nm, 10% laser intensity, 800 gains).

Rice pollen germination assay in vitro and in vivo

In vitro pollen germination was performed as described previously (Liu et al. 2016). Rice pollen grains were collected from flowering panicles into a liquid germination medium (20% [*w*/*v*] sucrose, 10% [*w*/*v*] polyethylene glycol 4000, 3 mM $Ca(NO_3)_2$•$4H_2O$, 40 mg L^{-1} H_3BO_3, and 3 mg L^{-1} vitamin B1) and cultured for 10 min at room temperature (30 °C) under moist conditions to generate synchronously germinated rice pollen grains. Pictures were taken using a light microscopy.

In vivo pollen tube growth was performed as described previously (Liu et al. 2016). In brief, rice pistils at 6 h after pollination were cut and fixed in Carnoy's solution overnight. Pistils were washed 5 times with water, softened by 1 M NaOH at 55 °C for 30 min, and stained in 0.1% (*w*/*v*) aniline blue (in 0.1 M K_2HPO_4, pH 8.5) at room temperature for 4 to 16 h in the dark. Fluorescent images were observed with Eclipse Ni-E microscope (Nikon) under UV light.

Gene editing and transgenic constructs

CRISPR-Cas9 knockout mutants of *OsAM1* in WT cv. Dongjing were obtained using the methods as previously described (Wang et al. 2017). For rice OsAM1 functional complementation and protein localization, an 8,986-bp promoter and coding region (without stop codon) was amplified from WT rice gDNA and fused with eYFP at the C-terminus, plus the WT 366-bp 3′-UTR. The final 10,108-bp fragment described above was inserted into the binary vector pCAMBIA1301 and transformed into *osam1*^{cas9} or *osinp1* (Zhang et al. 2020) calli to create the complementation and protein localization line. To observe OsINP1 and OsDAF1 protein localization in *osam1*^{cas9} mutant, *OsINP1pro:OsINP1-eYFP* and *OsDAF1pro:OsDAF1-eYFP* constructs described previously (Zhang et al. 2020) were used to transform *osam1*^{cas9} calli.

Sequence retrieval and phylogenetic analysis of the plant SRF proteins

Plant orthologs of OsAM1 were retrieved from the Phytozome database (https://phytozome.jgi.doe.gov/pz/portal.html) and NCBI BLASTP search using the OsAM1 protein sequence. Protein sequences with $E < e^{-60}$ or score > 300 were classified as OsAM1 orthologs, and BLAST results from algal species were used as phylogenetic roots ($E > e^{-40}$, score < 160). In total, 273 protein homologs from 44 plant species were retrieved and used for phylogenetic analysis: algae (5 species/5 sequences), mosses (5/16), ferns (3/9), common ancestor of angiosperm (3/10), sister lineage of monocot (5/32), grasses (6/61), sister lineage of eudicot (3/16), and eudicots (16/125).

Sequence alignment was performed using MEGA11 software with the ClustalW algorithm and default parameters. The phylogenetic tree was constructed using IQ-TREE (Trifinopoulos et al. 2016) with the maximum likelihood method, SH-aLRT test, and ultrafast bootstrap with 1,000 replicates and visualized using iTOL (https://itol.embl.de/) (Letunic and Bork 2021).

Subcellular localization assay

The coding region of OsAM1 was amplified and cloned into pHB-$35S_{pro}$-eGFP. The recombinant and empty vectors were transformed into *Agrobacterium tumefaciens* GV3101 as described previously (Zhang et al. 2020). In brief, the bacteria were collected and resuspended (A_{600} 0.6) in infection solution (10 mM MES, 10 mM $MgCl_2$, and 200 μM acetosyringone). The prepared suspensions were infiltrated into *N. benthamiana* leaves and grown in the dark for 36 h. For the plasmolysis assay, infiltrated leaves were treated with 30% (*w*/*v*) sucrose solution for 20 min before observation. Fluorescent signals were photographed using a Leica SP5 confocal microscope (Leica TCS SP5, excitation 488 nm, emission 500 to 550 nm, 10% laser intensity, 800 gains). All primers used are listed in Supplementary Table S2.

Y2H assay

The coding sequences of *AtINP1*, truncated *AtAM1*, and *OsAM1* were amplified and cloned into pGBKT7 or pGADT7 (Clontech). Constructs for *OsINP1* and truncated *OsDAF1* were described previously (Zhang et al. 2020). For OsINP1 truncation constructs, coding sequences of corresponding truncated fragments indicated in Supplementary Fig. S5 were amplified and cloned into pGBKT7 or pGADT7. These constructs were transformed into *Saccharomyces cerevisiae* strain AH109, and Y2H assays were performed via the Clontech kit according to the manufacturer's instructions. All primers used are listed in Supplementary Table S2.

BiFC assay

The coding regions of truncated *OsAM1* were amplified and each was cloned into pXY106-nYFP and pXY104-cYFP plasmid. Constructs for *OsINP1* and *OsDAF1* were described previously (Zhang et al. 2020). The recombinant vectors were cotransformed into *A. tumefaciens* GV3101 and infiltrated into *N. benthamiana* leaves as described above and grown in the dark for 48 h. Fluorescent eYFP signals were monitored using a Leica SP8 confocal microscope (Leica TCS SP8 X, excitation 514 nm; emission 522 to 555 nm, 10% laser intensity, 800 gains). Primers used are listed in Supplementary Table S2.

Split-luciferase assay

The coding region of truncated *OsAM1* was amplified, and each was cloned into p1300-nLuc and p1300-cLuc plasmid. Constructs for *OsINP1* and *OsDAF1* were described previously (Zhang et al. 2020). The recombinant vectors were cotransformed into *A. tumefaciens* GV3101 and infiltrated into *N. benthamiana* leaves as described above and grown in the dark for 40 h. The leaves were then sprayed with 5 mM luciferin and kept in the dark for 10 min. A cooling CCD imaging apparatus (Tanon-5200) was used for image capture.

Accession numbers

Sequence data from this article can be found in the GenBank/EMBL data libraries under accession numbers: OsAM1 (LOC_Os02g10110), OsINP1 (LOC_Os02g44250), and OsDAF1 (LOC_Os02g26160).

Acknowledgments

We thank Zhijing Luo, Mingjiao Chen, and Ting Luo for field management. We thank Xiaofei Chen for rice transformation. We thank Natalie Betts for language editing and writing suggestions.

Author contributions

X.Z. and Y.K. performed experiments and analyzed data. Q.T. participated in some experiments. W.L. and K.J. conceived the project. W.L. and X.Z. wrote the paper.

Supplementary data

The following materials are available in the online version of this article.

Supplementary Figure S1. Anther transverse sections of WT and osam1 plants.

Supplementary Figure S2. Subcellular localization of OsAM1.

Supplementary Figure S3. Schematic diagrams of truncated OsAM1 constructs for protein interaction assays.

Supplementary Figure S4. *osam1*^{cas9}*;osinp1* double mutant displays no additive phenotype.

Supplementary Figure S5. Different regions of OsINP1 interact with extracellular OsAM1 and intracellular OsDAF1.

Supplementary Figure S6. OsAM1 is the only member in rice SRF proteins that contain the eHR.

Supplementary Figure S7. Grass AM1 proteins likely to generally contain the eHR.

Supplementary Figure S8. Eudicot SRF2 proteins likely to not contain the eHR.

Supplementary Table S1. Amino acid sequence identity between OsAM1 and its orthologs from a variety of plant taxa.

Supplementary Table S2. List of primers used in this study.

Funding

This work was supported by grants from the National Natural Science Foundation of China (32200267 and 3231101074); the China Postdoctoral Science Foundation (2022M712079); and the Innovative Research Team, Ministry of Education, and 111 Project (Grant B14016).

Conflict of interest statement. None declared.

Data availability

All data generated or analyzed in this paper are presented in the main text, figures, Supplementary Figures, and tables or are available from the corresponding author upon request.

References

Afzal AJ, Wood AJ, Lightfoot DA. Plant receptor-like serine threonine kinases: roles in signaling and plant defense. *Mol Plant Microbe Interact*. 2008:21(5):507–517. https://doi.org/10.1094/MPMI-21-5-0507

Albert B, Ressayre A, Dillmann C, Carlson AL, Swanson RJ, Gouyon PH, Dobritsa AA. Effect of aperture number on pollen germination, survival and reproductive success in *Arabidopsis thaliana*. *Ann Bot*. 2018:121(4):733–740. https://doi.org/10.1093/aob/mcx206

Alcázar R, García AV, Kronholm I, De Meaux J, Koornneef M, Parker JE, Reymond M. Natural variation at strubbelig receptor kinase 3 drives immune-triggered incompatibilities between *Arabidopsis thaliana* accessions. *Nat Genet*. 2010:42(12):1135–1139. https://doi.org/10.1038/ng.704

Ariizumi T, Toriyama K. Genetic regulation of sporopollenin synthesis and pollen exine development. *Annu Rev Plant Biol*. 2011:62(1):437–460. https://doi.org/10.1146/annurev-arplant-042809-112312

Chaudhary A, Chen X, Gao J, Leśniewska B, Hammerl R, Dawid C, Schneitz K. The *Arabidopsis* receptor kinase STRUBBELIG regulates the response to cellulose deficiency. *PLoS Genet*. 2020:16(1):1–27. https://doi.org/10.1371/journal.pgen.1008433

Chevalier D, Batoux M, Fulton L, Pfister K, Yadav RK, Schellenberg M, Schneitz K. STRUBBELIG defines a receptor kinase-mediated signaling pathway regulating organ development in *Arabidopsis*. *Proc Natl Acad Sci U S A*. 2005:102:9074–9079. https://doi.org/10.1073/pnas.0503526102

De Smet I, Voß U, Jürgens G, Beeckman T. Receptor-like kinases shape the plant. *Nat Cell Biol*. 2009:11(10):1166–1173. https://doi.org/10.1038/ncb1009-1166

Dobritsa AA, Coerper D. The novel plant protein INAPERTURATE POLLEN1 marks distinct cellular domains and controls formation of apertures in the *Arabidopsis* pollen exine. *Plant Cell*. 2012:24(11):4452–4464. https://doi.org/10.1105/tpc.112.101220

Dobritsa AA, Kirkpatrick AB, Reeder SH, Li P, Owen HA. Pollen aperture factor INP1 acts late in aperture formation by excluding specific membrane domains from exine deposition. *Plant Physiol*. 2018:176(1):326–339. https://doi.org/10.1104/pp.17.00720

Dobritsa AA, Reeder SH. Formation of pollen apertures in *Arabidopsis* requires an interplay between male meiosis, development of INP1-decorated plasma membrane domains, and the callose wall. *Plant Signal Behav*. 2017:12(12):1–4. https://doi.org/10.1080/15592324.2017.1393136

Edlund AF. Pollen and stigma structure and function: the role of diversity in pollination. *The Plant Cell Online*. 2004:16(suppl_1):S84S97. https://doi.org/10.1105/tpc.015800

El-Ghazaly G, Jensen WA. Studies of the development of wheat (*Triticum aestivum*) pollen. *Grana*. 1986:25(1):1–29. https://doi.org/10.1080/00173138609429929

Eyüboglu B, Pfister K, Haberer G, Chevalier D, Fuchs A, Mayer KF, Schneitz K. Molecular characterisation of the STRUBBELIG-RECEPTOR FAMILY of genes encoding putative leucine-rich repeat receptor-like kinases in *Arabidopsis thaliana*. *BMC Plant Biol*. 2007:7(1):16. https://doi.org/10.1186/1471-2229-7-16

Furness CA, Rudall PJ. Pollen aperture evolution—a crucial factor for eudicot success? *Trends Plant Sci*. 2004:9(3):154–158. https://doi.org/10.1016/j.tplants.2004.01.001

Gao J, Chaudhary A, Vaddepalli P, Nagel MK, Isono E, Schneitz K. The *Arabidopsis* receptor kinase STRUBBELIG undergoes clathrin-dependent endocytosis. *J Exp Bot*. 2019:70(15):3881–3894. https://doi.org/10.1093/jxb/erz190

Jeon J, Lee S, Jung K, Jun S, Jeong D, Lee J, Kim C, Jang S, Lee S, Yang K, *et al.* T-DNA insertional mutagenesis for functional genomics in rice. *Plant J*. 2000:22(6):561–570. https://doi.org/10.1046/j.1365-313x.2000.00767.x

Just TH, Wodehouse RP. *Pollen grains, their structure, identification and significance in science and medicine*. South Bend: American Midland Naturalist; 1936.

Katifori E, Alben S, Cerda E, Nelson DR, Dumais J. Foldable structures and the natural design of pollen grains. *Proc Natl Acad Sci U S A*. 2010:107(17):7635–7639. https://doi.org/10.1073/pnas.0911223107

Köhler E, Lange E. A contribution to distinguishing cereal from wild grass pollen grains by LM and SEM. *Grana*. 1979:18(3):133–140. https://doi.org/10.1080/00173137909424973

Kwak S, Shen R, Schiefelbein J. Positional signaling mediated by a receptor-like kinase in *Arabidopsis*. *Science*. 2005:1:1111–1114. https://doi.org/10.1126/science.1105373

Lee BH, Wang R, Moberg IM, Reeder SH, Amom P, Tan MH, Amstutz K, Chandna P, Helton A, Andrianova EP, *et al*. A species-specific functional module controls formation of pollen apertures. *Nat Plants*. 2021:7(7):966–978. https://doi.org/10.1038/s41477-021-00951-9

Lee BH, Weber ZT, Zourelidou M, Hofmeister BT, Schmitz RJ, Schwechheimer C, Dobritsa AA. *Arabidopsis* protein kinase D6PKL3 is involved in the formation of distinct plasma membrane aperture domains. *Plant Cell*. 2018:30(9):2038–2056. https://doi.org/10.1105/tpc.18.00442

Letunic I, Bork P. Interactive Tree of Life (iTOL) v5: an online tool for phylogenetic tree display and annotation. *Nucleic Acids Res*. 2021:49(W1):W293–W296. https://doi.org/10.1093/nar/gkab301

Li P, Ben-Menni Schuler S, Reeder SH, Wang R, Suárez Santiago VN, Dobritsa AA. INP1 involvement in pollen aperture formation is evolutionarily conserved and may require species-specific partners. *J Exp Bot*. 2018:69(5):983–996. https://doi.org/10.1093/jxb/erx407

Li F-S, Phyo P, Jacobowitz J, Hong M, Weng J-K. The molecular structure of plant sporopollenin. *Nat Plants*. 2019:5(1):1–128. https://doi.org/10.1038/s41477-018-0353-0

Lin L, Zhong SH, Cui XF, Li J, He ZH. Characterization of temperature-sensitive mutants reveals a role for receptor-like kinase SCRAMBLED/STRUBBELIG in coordinating cell proliferation and differentiation during *Arabidopsis* leaf development. *Plant J*. 2012:72(5):707–720. https://doi.org/10.1111/j.1365-313X.2012.05109.x

Liu L, Zheng C, Kuang B, Wei L, Yan L, Wang T. Receptor-like kinase RUPO interacts with potassium transporters to regulate pollen tube growth and integrity in rice. *PLoS Genet*. 2016:12(7):1–23. https://doi.org/10.1371/journal.pgen.1006085

Ma H. Molecular genetic analyses of microsporogenesis and microgametogenesis in flowering plants. *Annu Rev Plant Biol*. 2005:56(1):393–434. https://doi.org/10.1146/annurev.arplant.55.031903.141717

Mccormick S. Control of male gametophyte development. *Plant Cell*. 2004:16(suppl_1):142–154. https://doi.org/10.1105/tpc.016659

Platre MP, Satbhai SB, Brent L, Gleason MF, Cao M, Grison M, Glavier M, Zhang L, Gaillochet C, Goeschl C, *et al*. The receptor kinase SRF3 coordinates iron-level and flagellin dependent defense and growth responses in plants. *Nat Commun*. 2022:13(1):4445. https://doi.org/10.1038/s41467-022-32167-6

Plourde SM, Amom P, Tan M, Dawes AT, Dobritsa AA. Changes in morphogen kinetics and pollen grain size are potential mechanisms of aberrant pollen aperture patterning in previously observed and novel mutants of *Arabidopsis thaliana*. *PLoS Comput Biol*. 2019:15(2):e1006800. https://doi.org/10.1371/journal.pcbi.1006800

Quilichini TD, Grienenberger E, Douglas CJ. The biosynthesis, composition and assembly of the outer pollen wall: a tough case to crack. *Phytochemistry*. 2015:113:170–182. https://doi.org/10.1016/j.phytochem.2014.05.002

Shi J, Cui M, Yang L, Kim YJ, Zhang D. Genetic and biochemical mechanisms of pollen wall development. *Trends Plant Sci*. 2015:20(11):741–753. https://doi.org/10.1016/j.tplants.2015.07.010

Shiu S-H, Bleecker AB. Receptor-like kinases from *Arabidopsis* form a monophyletic gene family related to animal receptor kinases. *Proc Natl Acad Sci*. 2001:98(19):10763–10768. https://doi.org/10.1073/pnas.181141598

Tor M, Lotze MT, Holton N. Receptor-mediated signaling in plants: molecular patterns and programmes. *J Exp Bot*. 2009:60(13):3645–3654. https://doi.org/10.1093/jxb/erp233

Trifinopoulos J, Nguyen L-T, von Haeseler A, Minh BQ. W-IQ-TREE: a fast online phylogenetic tool for maximum likelihood analysis. *Nucleic Acids Res*. 2016:44(W1):W232–W235. https://doi.org/10.1093/nar/gkw256

Vaddepalli P, Fulton L, Batoux M, Yadav RK, Schneitz K. Structure-function analysis of strubbelig, an *Arabidopsis* atypical receptor-like kinase involved in tissue morphogenesis. *PLoS One*. 2011:6:e19730. https://doi.org/10.1371/journal.pone.0019730

Vieira AM, Feijó JA. Hydrogel control of water uptake by pectins during in vitro pollen hydration of *Eucalyptus globulus*. *Am J Bot*. 2016:103(3):437–451. https://doi.org/10.3732/ajb.1500373

Wang R, Dobritsa A. Exine and aperture patterns on the pollen surface: their formation and roles in plant reproduction. *Ann Plant Rev*. 2018:1:589–628. https://doi.org/10.1002/9781119312994.apr0625

Wang C, Higgins JD, He Y, Lu P, Zhang D, Liang W. Resolvase OsGEN1 mediates DNA repair by homologous recombination. *Plant Physiol*. 2017:173(2):1316–1329. https://doi.org/10.1104/pp.16.01726

Zhang D, Luo X, Zhu L. Cytological analysis and genetic control of rice anther development. *J Genet Genomics*. 2011:38(9):379–390. https://doi.org/10.1016/j.jgg.2011.08.001

Zhang X, Zhao G, Tan Q, Yuan H, Betts N, Zhu L, Zhang D, Liang W. Rice pollen aperture formation is regulated by the interplay between OsINP1 and OsDAF1. *Nat Plants*. 2020:6(4):394–403. https://doi.org/10.1038/s41477-020-0630-6

Zhou Y, Amom P, Reeder SH, Lee BH, Helton A, Dobritsa AA. Members of the ELMOD protein family specify formation of distinct aperture domains on the *Arabidopsis* pollen surface. *eLife*. 2021:10:e71061. https://doi.org/10.7554/eLife.71061

Zhou Y, Dobritsa AA. Formation of aperture sites on the pollen surface as a model for development of distinct cellular domains. *Plant Sci*. 2019:288:110222. https://doi.org/10.1016/j.plantsci.2019.110222